

## Wavelength-dependent spatial variation in the reflectance of ‘homogeneous’ ground calibration targets.

V. Salvatori<sup>†</sup>, P.M. Atkinson<sup>‡</sup>, E.J. Milton<sup>‡</sup>, D.R. Emery<sup>†</sup>

<sup>†</sup> NERC Equipment Pool for Field Spectroscopy, University of Southampton, Highfield, Southampton SO17 1BJ. E-mail: [vs497@soton.ac.uk](mailto:vs497@soton.ac.uk), [epfs@soton.ac.uk](mailto:epfs@soton.ac.uk)

<sup>‡</sup> Dept. of Geography, University of Southampton, Highfield, Southampton SO17 1BJ. E-mail: [pma@soton.ac.uk](mailto:pma@soton.ac.uk), [ejm@soton.ac.uk](mailto:ejm@soton.ac.uk)

### Introduction

Remotely sensed data are most useful if calibrated to spectral reflectance of known features. One simple method of calibration is regression of remote data on the reflectance of several ground targets as measured in the field, the so called empirical line method (ELM). The ideal situation would be one where a range of ground targets representing all the features of interest in the remote image were available for ground measurements (Lawless et al., 1998). The identification of suitable ground targets is constrained by several limitations, such as their size (to minimise edge effects), their absolute reflectance (to represent spectral characteristics of the image) and their effective spatial variability (to extract reflectance characteristics representative of the target). The size of a ground target is dependent on the spatial resolution of the image that must be calibrated (Justice & Townshend, 1981) and the number of observations needed to represent features in the image has been suggested to depend upon the spatial resolution of the remotely sensed image (Justice & Townshend, 1981) and on the spatial variability of the ground target (Harlan et al., 1979; Curran & Williamson, 1986). Although ground targets used for calibration should be spectrally “bland” and spatially uniform by definition (Clark et al., 1999), it is sometimes very difficult to find such places available for calibrating remotely sensed images. When surfaces that apparently satisfy these conditions are available in suitable size, their sampling needs to be designed to optimise representation of the whole surface and available resources (e.g., effort and time).

Surfaces that look spatially uniform by eye may actually contain spatial variation, and this spatial variation may depend on wavelength (Atkinson & Emery, 1999). Such variability can be detected using geostatistics, which is concerned with issues such as spatial correlation and analyses of spatial data. Geostatistical tools have been used in a variety of studies and the variogram has been applied in remote sensing and ecology to design optimal sampling strategies for variables sampled in space (Atkinson, 1991; Rossi et al., 1992) and time (Salvatori et al., 1999).

This study investigates the spatial variability of potentially suitable ground calibration targets (GCT) using a geostatistical approach, which gives results that can be used to design optimal sampling strategies for such surfaces. The targets were selected from an area where an Itres Instruments Compact Airborne Spectral Imager (*casi*) with ground resolution of about 1.5 metres was flown at the same time as ground data were acquired.

### *The variogram function*

On average, observations close together in space are more likely to be similar than those that are further apart, a phenomenon . Spatial continuity tools such as the variogram are used to infer the spatial autocorrelation based on random function theory (Journel & Huijbregts, 1978). Let  $z(\mathbf{x})$  represent the value of a variable at location  $\mathbf{x}$  and let  $z(\mathbf{x} + \mathbf{h})$  represent the value of the same variable at some  $\mathbf{h}$  distance and direction (or lag) away. The semi-variance is a function describing half of the expected squared differences between  $z(\mathbf{x})$  and  $z(\mathbf{x} + \mathbf{h})$ . The semi-variogram (most commonly just the variogram) function summarises the spatial continuity for all possible pairings of data for all lag distances  $\mathbf{h}$  as:

$$\hat{\gamma}(\mathbf{h}) = \frac{1}{2n(\mathbf{h})} \sum_{i=1}^{n(\mathbf{h})} [z(\mathbf{x}_i) - z(\mathbf{x}_i + \mathbf{h})]^2$$

where  $\hat{\gamma}(\mathbf{h})$  indicates that these are experimental semi-variance values derived only for a number of discrete distance classes and  $n(\mathbf{h})$  the number of pairs of points separated by a lag  $\mathbf{h}$ .

Mathematical models are fitted to experimental variograms to describe their behaviour. The empirical distributions are described by three parameters (Fig.1):

- The nugget variance  $C_0$ . This is the y-intercept, usually non-zero, and can be attributed to measurement errors and unresolved spatial variation;
- The range  $a$ . This is the lag at which statistical correlation between data is zero and variability can be considered purely random. It represents the scale of variation of the data;
- The sill  $C$ . This is the corresponding variance found for pairs separated by lags greater than the range. It can be decomposed into two factors  $c_0$  and  $c_1$ . The former is the nugget, the latter can be considered as structured variation.

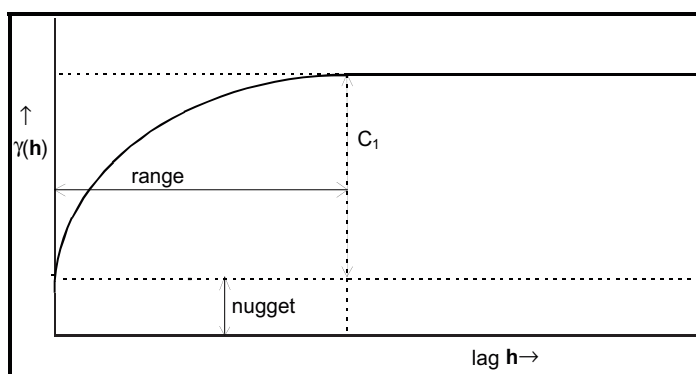


Figure 1 – Variogram parameters

Commonly used models fitted to experimental variograms are described in Isaaks & Srivastava (1989) and Cressie (1993).

### Study site

Data were acquired in the field on surfaces within a disused airfield on Thorney Island, West Sussex, UK. The site is characterised by areas of visually homogeneous surfaces such as asphalt roads, concrete bases, grass fields and some buildings. The spatial structure of the whole area is such that relatively large surfaces can be identified at a distance that can ensure the avoidance of light scattering by vertical surfaces such as buildings and walls.

Three surfaces were considered as GCTs: asphalt, concrete and grass. The asphalt surface was represented by a straight road of 2,000 m of length and 50 m width; the concrete surface consisted of blocks of slightly irregular size, where a total of 7 columns by 30 rows could be identified, and between each block a thin line of bitumen may be present; the grass field was homogeneously composed by monocotyledon species and data were acquired prior to the flowering season.

### Data collection

A pilot study was conducted on the concrete surface, where data were acquired both randomly and systematically. The results of the pilot study showed that spatial structure existed (Salvatori, 1999) and thus systematic sampling was more appropriate for such a surface. Following from the results of the pilot study, systematic sampling was carried out on the asphalt, concrete and grass surfaces.

To check for any spatial pattern of variability three line-transects, one for each surface, were selected and reflectance data were recorded at points separated by 1.5 metres. Transects were placed at least 15 metres from the edges of the surfaces.

Reflectance data were recorded with a field portable spectro-radiometer (ASD Fieldspec FR<sup>TM</sup>). The instrument records radiance over the visible to the short-wave infra-red regions of the electromagnetic spectrum with a spectral sampling of 1.4 nm in the range between 350 to 2500 nm. The instrument operates in single-beam mode and is controlled by a sub-notebook computer. An 8° optic was mounted on a hand-held mast and the readings were standardised to a 99% reflective Spectralon<sup>TM</sup> Panel.

The field campaign was conducted on 6<sup>th</sup> October 1999 at near-noon time. Sky conditions were clear with some thin cirruses, and sampling activities lasted for about three hours.

The data along the transects were acquired at 3.6 metres above the surface, obtaining a field-of-view (FOV) with a diameter of 50 cm.

### Data pre-processing

Data were processed to produce values of absolute reflectance for each sample. As the purpose of the study was to define the optimal sampling strategy to calibrate *casi* data, only the region of the electromagnetic spectrum corresponding to the wave bands of *casi* were considered for further analysis.

Subsequently, the data were filtered to produce spectral bands corresponding to the 13 bands of the *casi* instrument. Filters were square bandpass so the relative spectral response is 1 in all wavelengths between the start and end. The wavelength ranges for each band are reported in table 1.

Band No	1	2	3	4	5	6	7	8	9	10	11	12	13
nm start	403.5	432.9	479.2	499.6	544.4	569.4	680.3	697.4	745.0	760.3	766.0	815.8	846.5
nm end	422.2	453.6	500.0	520.5	565.4	680.6	686.3	703.4	758.7	766.3	785.5	825.7	885.3

Table 1. – Wavelength ranges in *casi* bands.

### Data processing

The mean and standard deviation of each band in the longitudinal transects were computed and tested for heteroscedasticity (Sokal & Rohlf, 1995). The spatial variation of each series (where a series is represented by the transect where reflectance was recorded on a specific band) was then represented by the variogram function.

Variograms were computed using the Gstat software (Pebesma and Wesseling, 199?). Model fitting was performed using a weighted least squares approach.

### Results

The mean reflectance of the three surfaces is showed in figs. 2-4, where the data recorded are represented for each surface.

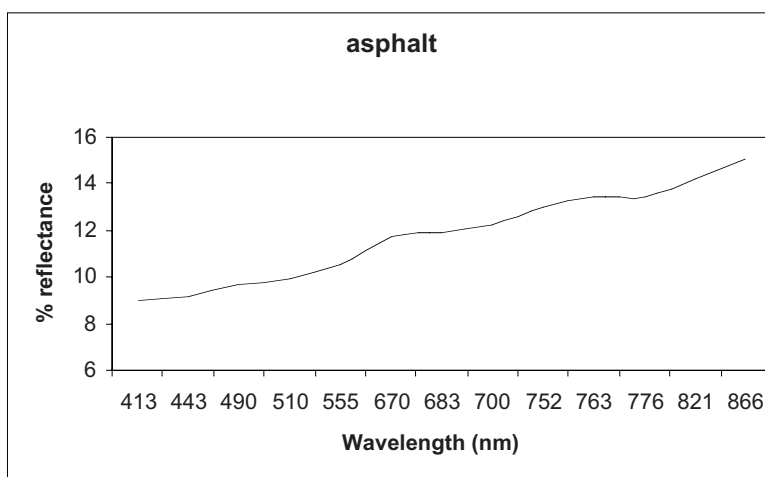


Fig. 2. - Mean reflectance for the asphalt surface

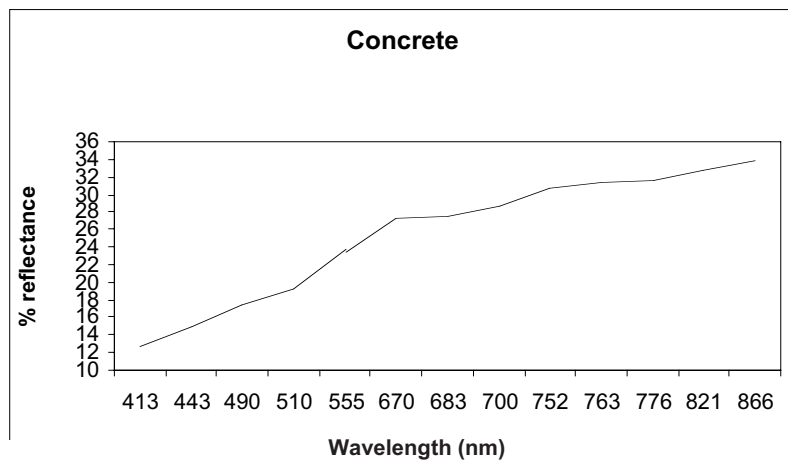


Fig. 3. - Mean reflectance for the concrete surface

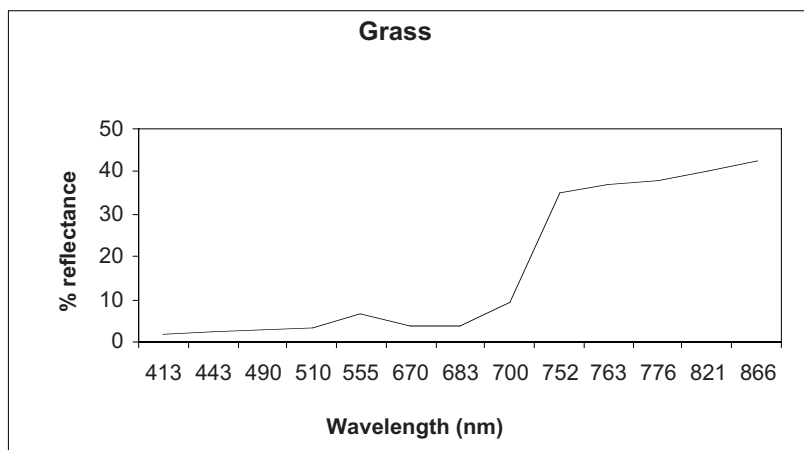


Fig. 4.- Mean reflectance for the grass surface

The three series showed higher values of variance at longer wavelengths and were significantly heteroscedastic ( $F_{max}$  ranging from 3.28, d.f. = 13, 98, to 216.1, d.f. = 13, 102,  $p$  always  $\ll 0.001$ ).

The presence of heteroscedasticity suggested that standardising the data by their mean would result in a drastic decrease of the between-series variance. Table 2 reports values of standard deviation for the three series and the respective values when data were standardised.

Casi band	Asphalt		Concrete		Grass	
	Raw	Stand	Raw	Stand	Raw	Stand
1	0.76	0.08	2.22	0.18	0.35	0.17
2	0.78	0.09	2.52	0.17	0.39	0.17
3	0.84	0.09	2.89	0.17	0.48	0.18
4	0.87	0.09	3.09	0.16	0.56	0.17
5	0.94	0.09	3.56	0.15	0.97	0.14
6	1.04	0.09	4.14	0.15	0.84	0.22
7	1.07	0.09	4.19	0.15	0.86	0.22
8	1.10	0.09	4.23	0.15	1.37	0.15
9	1.18	0.09	4.35	0.14	4.45	0.13
10	1.25	0.09	4.45	0.14	4.73	0.13
11	1.23	0.09	4.40	0.14	4.82	0.13
12	1.28	0.09	4.38	0.13	4.99	0.12
13	1.38	0.09	4.36	0.13	5.19	0.12

Tab. 2.- Standard deviation for samples collected on asphalt, concrete and grass. For each surface the values resulting from raw and standardised-by-the-mean (Stand) data are given.

### Asphalt

Variograms were estimated for the 13 casi bands. When plotted, they showed that values of variance increased with wavelength (fig. 5A). This would suggest that spatial variability is dependent on wavelength. Nevertheless, when the variograms were computed from the standardised data the effect of wavelength disappeared (fig. 5B).

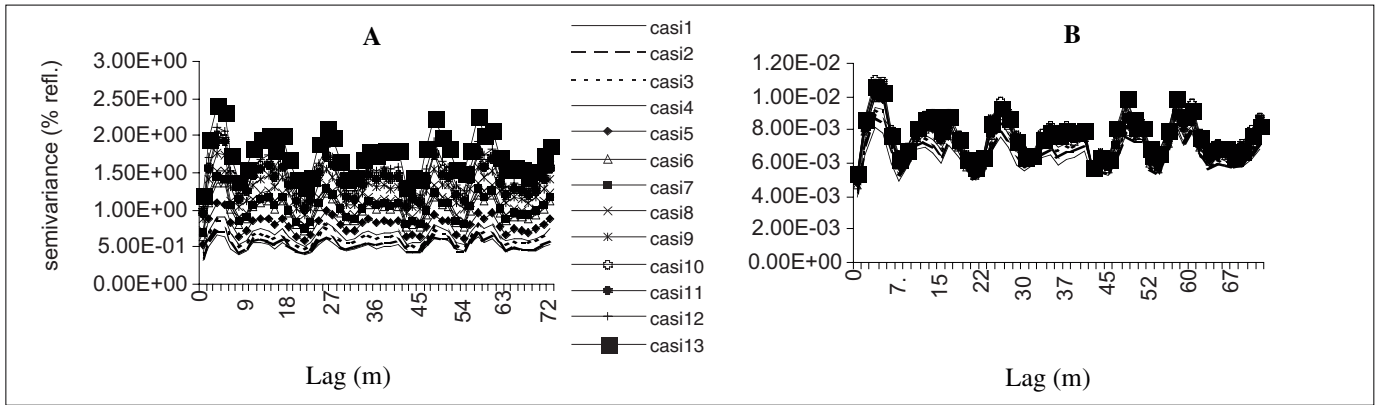


Figure 5.- Experimental variograms for the asphalt surface. A) Variograms computed from raw data and B) from data standardised by the mean.

In this situation, only one variogram could be computed from reflectance values recorded at any wavelength within the range considered as spatial patterns affected all wavelengths similarly. This spectral stability makes the asphalt surface a potentially suitable GCT (Lawless et al., 1998). These results suggest that recording reflectance in a wavelength corresponding to one single band of the casi would be enough to characterise the target spatial variability.

Mathematical models were fitted to the experimental variograms to define the three variogram parameters that best represented the experimental data. The model fitted was the linear plus sill model for all wavelengths. The parameters describing the amount of variability (i.e., nugget and sill) assumed lower values for variograms produced by standardised data (fig. 6).

This is an expected result, as the overall variability was lowered by the standardisation process. It is interesting to note that standardising the data does not affect the scale of spatial variation, as the range assumed exactly the same values for the two series (fig. 6).

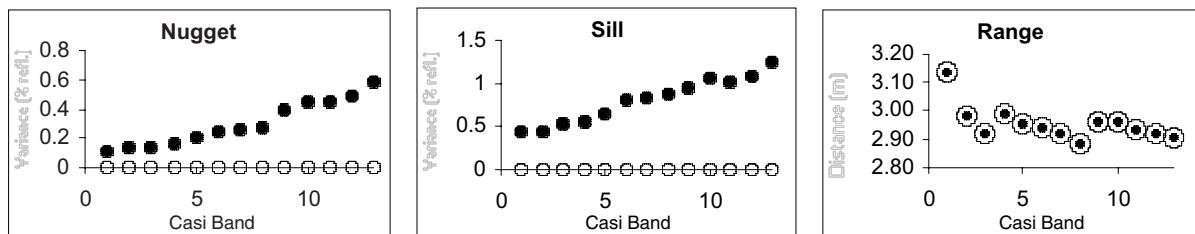


Fig. 6.- Variogram parameters for the asphalt surface in the 13 casi bands. Filled and empty dots are relative to models fitted to variograms from raw data and from standardised data, respectively.

Mean values of nugget and sill (from raw and standardised data, respectively) were 0.29 ( $\pm 0.15$  SD) and 0.002 ( $\pm 0.0004$  SD) and 0.80 ( $\pm 0.26$  SD) and 0.006 ( $\pm 0.0002$  SD), respectively. The scale of variation showed that only subsequently recorded data were autocorrelated, as the sill was reached at a distance in space < than 2 intervals (mean range = 2.95 metres). The wavelength effect on the scale of variation seems to be irrelevant, being the SD = 0.06 metres.

**Concrete**

The variograms resulting from data collected on the concrete surface showed similar behaviour to those relative to the asphalt target, but a more pronounced spatial structure was detected. As previously detected for the asphalt surface, variance seems to increase with wavelength (fig. 7A). This effect is considerably attenuated when the variograms are computed from data standardised by the mean (fig. 7B).

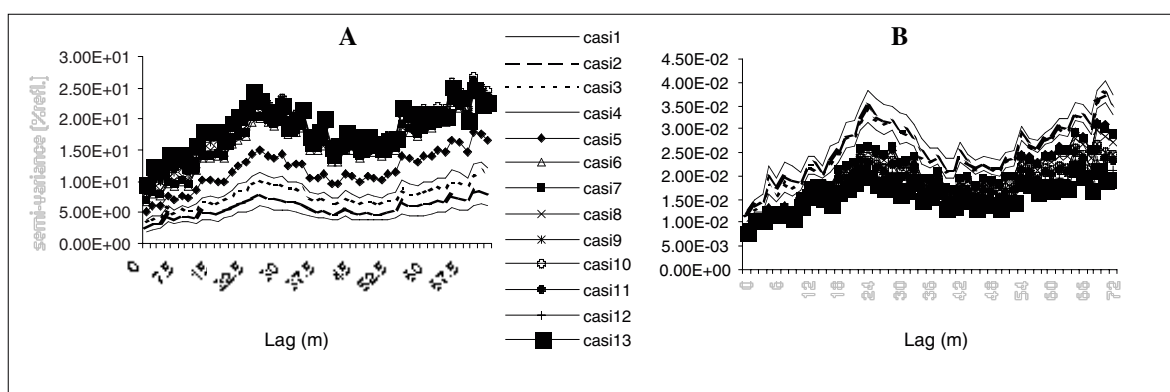


Figure 7.- Experimental variograms for the concrete surface. A) Variograms computed from raw data and B) from data standardised by the mean.

Although some differences were still apparent after the data were standardised, the wavelength-related variability can be ignored. The structured and *a priori* variances (i.e., those represented by the sill and the nugget) and data collected on one single band can be considered to be representative of the whole set of the *casi* bands since variability between the coefficients of the fitted models is very low. The model fitted was the spherical and the coefficients obtained are sketched in fig. 8.

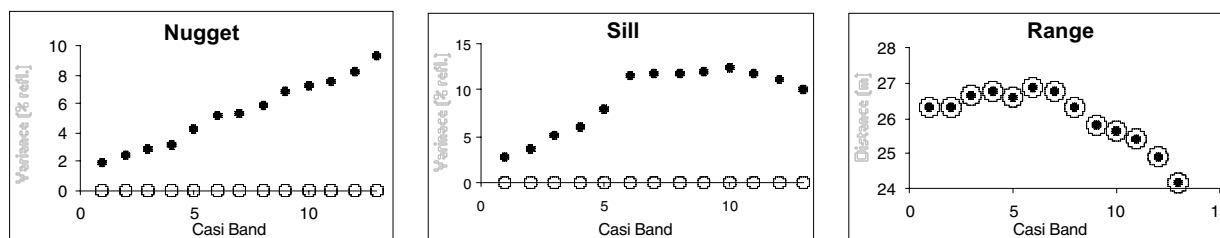


Fig. 8.- Variogram parameters for the concrete surface in the 13 *casi* bands. Filled and empty dots are relative to models fitted to variograms from raw data and from standardised data, respectively.

The average values of nugget for raw and standardised data were  $5.39 (\pm 2.35 \text{ SD})$  and  $0.008 (\pm 0.002 \text{ SD})$ , respectively, while the sill averaged  $9.06 (\pm 3.51 \text{ SD})$  and  $0.014 (\pm 0.002 \text{ SD})$ . Although the SD takes very low values for parameters describing models fitted to variograms computed from standardised data, it is worth noticing that such values are of one order of magnitude higher than those recorded for the analogous parameters in the asphalt surface.

The scale of spatial variability averaged  $26.04 \text{ m} (\pm 0.82 \text{ SD})$ . This high value of range may be explained with the structural composition of the concrete surface, made up of blocks of about  $6 \times 6 \text{ m}$  of size. The presence of blocks composed of slightly different material resulted in an irregular sequence of brighter and darker blocks that may affect the spatial variability of reflectance. The range seems to be affected by the wavelength factor, showing a relatively high SD. However, the scale of variation between wavelengths is smaller than the spatial resolution of the *casi* image, thus it can be assumed to be irrelevant. The structure of the concrete surface, with many minor inclusions and the presence of a line of bitumen, sometimes also associated with small amount of vegetative material, in between the blocks, certainly contributes to such a result.

## Grass

Data were acquired on a grass field that was homogeneous at species level and not affected by anthropogenic activities such as mowing. The grass height was about 25 cm.

The variograms resulting from the reflectance recorded on the grass field showed a characteristic difference in behaviour related to two regions of the EM spectrum. *Casi* bands 1 to 8 assumed very low values of variance while the remaining 5 showed much higher structured variance (fig. 9A).

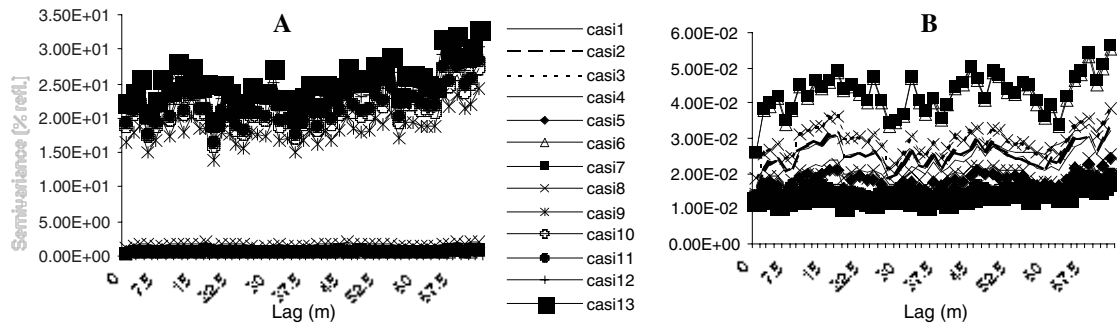


Figure 9.- Experimental variograms for the grass field. A) Variograms computed form raw data and B) from data standardised by the mean.

The separation of the *casi* bands into two groups coincides with two regions of the EM spectrum separated by the near-IR region. This region is known as the red-edge. A similar behaviour of variograms computed from reflectance recorded on transects over vegetated surfaces has been reported by Atkinson & Emery (1999), who described the presence of a “fundamental difference between spatial variation in the visible and near-infrared wavelengths” for heathland in southern England, UK. In such a situation, standardising the data by their sample mean does not make things clearer. On the contrary, it obscures patterns that are clearly visible from variograms of raw data (fig. 9B). For this target it is evident that ground data must be recorded at least in two wavelengths, belonging to the two regions of the EM spectrum; visible and near-IR.

The models fitted to the experimental variograms confirmed the existence of such two regions (Fig. 10).

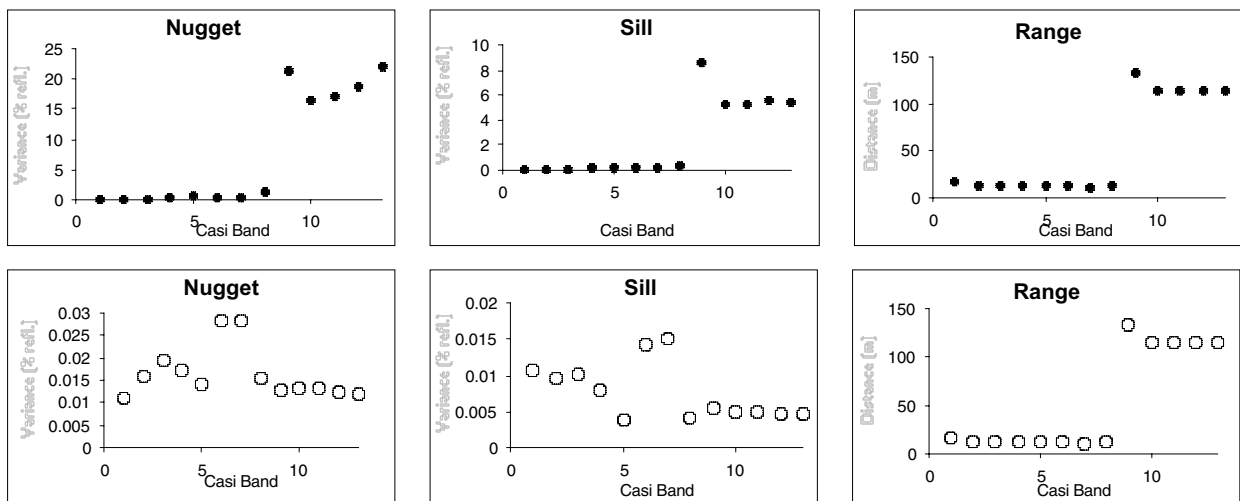


Fig. 10.- Variogram parameters for the grass field in the 13 *casi* bands. Upper series is relative to raw data, while lower one is relative to standardised data.

It is interesting to note that variogram coefficients obtained from standardised data enhanced the detectability of different spatial scales of variation through the range, while tended to decrease the differences in structural variation and nugget. Nevertheless, in the graphs of the latter two parameters, the behaviour of reflectance recorded at wavelengths corresponding to the red-edge (see fig. 4) is underlined by the exceptionally high values of variance assumed by *casi* bands 6 and 7.

Average nugget, sill and range for bands 1 to 8 were 0.40 ( $\pm 0.41$  SD), 0.15 ( $\pm 0.11$  SD) and 12.9 metres ( $\pm 1.63$  SD), respectively. For bands 9 to 13 the three parameters assumed average values of 19.09 ( $\pm 2.48$  SD), 5.98 ( $\pm 1.40$  SD) and 118.5 ( $\pm 8.51$  SD).

### Conclusions

Calibration of remotely sensed images to surface reflectance is inherently simple in concept, yet is complex in practice because of the many effects that need to be taken into account (Clark et al., 1999). In this study we showed how the variogram can be helpful in detecting both the amount of variation and the scale of variation of potentially suitable GCTs. The variogram coefficients as

estimated by model fitting can then be used to design the sampling methodology and effort. The range gives an idea of the minimum distance required for data not to be autocorrelated.

The variogram function can be used in optimising sampling design for estimating the kriging variance that may be acceptable for a given survey (Burgess et al., 1981; Atkinson & Emery, 1999; McBratney et al., 1981).

We highlighted an aspect that may be underestimated when considering potentially suitable GCTs that look spatially homogeneous to the eye. Targets that look spatially homogeneous may in fact exhibit marked spatial variation. This spatial structure has implications for how such calibration targets should be sampled in field. Importantly, it is unlikely that a single observation will be sufficient to represent such variability. Further, where this spatial variation is wavelength dependent (e.g., for the grass field) more than one sampling strategy may need to be developed. The design of optimal strategies into which to sample such targets will be the subject of future research.

### Acknowledgments

We are grateful to W. Damon, G. Llewellyn and N. Hamm for assistance during field data collection.

### Literature cited

- Atkinson P.M. 1991. Optimal ground-based sampling for remote sensing investigations: estimating the regional mean. *Int. J. Remote Sensing*, 12: 559-567.
- Atkinson P.M. and Emery D.R. 1999. Exploring the relation between spatial structure and wavelength: implications for sampling reflectance in the field. *Int. J. Remote Sensing*, 20: 2663-2678.
- Burgess T.M., Webster R. and McBratney A.B. 1981. Optimal interpolation and isarithmic mapping of soil properties IV. Sampling strategy. *Journal of Soil Science*, 32: 643-659.
- Clark R.N., Swayze G.A., King T.V.V., Livo K.E., Kokaly R.F., Dalton J.B., Vance J.S., Rockwell B.W. and McDougal R.R. 1999. Surface reflectance Calibration of Terrestrial Imaging Spectroscopy Data. A tutorial using AVIRIS. Available at the following web site: <http://speclab.cr.usgs.gov/PAPERS/calibration/tutorial/calibntA.html>
- Cressie N.A.C. 1993. *Statistics for Spatial Data*. Revised Edition, New York: Wiley.
- Curran P.J. and Williamson H.D. 1986. *The Use of Remotely Sensed multispectral Data to Estimate the Green LAI of Grassland Canopies*, Report to the NERC grant GR3/5096.
- Harlan J.C., Deering D.H., Hass R.H. and Boyd H.E. 1979. Determination of range biomass using Landsat, in *Proceedings 13<sup>th</sup> International Symposium on Remote Sensing on Environment*, University of Michigan, Ann Arbor, pp. 659-672.
- Isaaks E. and Srivastava R.M. 1989. *An Introduction to Applied Geostatistics*, Oxford. Oxford Univ. Press.
- Journel A. and Huijbregts C. 1978. *Mining Geostatistics*, London. Academic Press.
- Justice C.O. and Townshend, J.R.G. 1981. in *Terrain Analysis and Remote Sensing* (J.R.G. Townshend Ed.), Allen and Unwin, London and Boston, pp. 38-58.
- Lawless K.P., Milton E.J. and Anger C.O. 1998. Investigation of changes in the reflectance of ground calibration targets (asphalt and concrete). *Information for Sustainability: 27<sup>th</sup> International Symposium on Remote Sensing of Environment*, ERIM, Ann Arbor, Michigan, 597-600
- McBratney A.B., Webster R. and Burgess T.M. 1981. The design of optimal sampling schemes for local estimation and mapping of regionalised variables I and II. *Computer & Geosciences*, 7: 331-345.
- Pebesma E.J. and Wesseling C.G. 1998. Gstat: a program for geostatistical modelling, prediction and simulation. *Computers & Geosciences*, 24: 17-31.
- Rossi R.E., Mulla D.J., Journel A.G. and Franz E.H. 1992. Geostatistical tools for modeling and interpreting ecological spatial dependence. *Ecological Monographs*, 62: 277-314.
- Salvatori V. 1999. Practical guidelines for the application of geostatistical techniques to sampling target surfaces. NERC EPFS Project Report. Sept. 1999.
- Salvatori V., Skidmore A.K., Corsi F. and van der Meer F. 1999. Estimating temporal independence of radio-telemetry data on animal activity. *J. Theor. Biology*, 198: 567-574.
- Sokal R.R. and Rohlf F.J. 1995. *Biometry* 3<sup>rd</sup> Edn. New York: W.H. Freeman & Co.